# The Influence of Corona on the Lightning Surge Propagation Along Transmission Lines

Milan Ignjatović, Jovan Cvetić, and Dragan Pavlović

*Abstract* – **Corona is the partial discharge that occurs around the wires and edges in inhomogeneous electric field. Minimum intensity of the electric field for the impact ionization of the gas is around 2.6 MV/m in dry air. In power systems, the corona is the unwanted effect caused by overvoltages. In this study the propagation of the overvoltage wave due to negative lightning along the transmission line is numerically simulated. The effect of the corona is modelled by the drift-diffusion-reaction equations for the electrons, the positive and the negative ions.**

*Keywords* – **Corona, Lightning overvoltage, Transmission lines, QV curve, Streamers.**

## I. INTRODUCTION

The lightning strike is one of the most common causes of power interruption on transmission lines and substations. Since it is a natural phenomenon, lightning occurrence can not be foreseen, but its performance on power systems can be estimated. The insulation strength is selected to minimize the risk of the failure, taking into account the statistical data of the lightning occurrence in the wider area and the cost of the insulation construction [1]. There are methods to estimate the magnitude and steepness of the average incoming surge that arrives at substations [2].

When the lightning strikes the transmission lines, two initiating events can happen - the shielding failure and the backflash. The shielding failure occurs when the lightning hits the phase conductor directly avoiding the shield wire. If the lightning hits the shield wire, the injected overvoltage can be greater than the critical flashover voltage of the insulation and the backflash occurs.

For the direct lightning strikes the main effect that influence the shape of the overvoltage waveform is the corona. It is a partial discharge that occurs around the conducting wire when the voltage is above the corona inception threshold described by the Peek's formula [3]. The corona effects the delay of the part of the impulse that is above the corona threshold and the attenuation of the overvoltage amplitude due to losses in the ionized gas in the area around the wire.

Milan Ignjatović is with the School of Electrical Engineering, University of Belgrade, 73 Bulevar kralja Aleksandra, 11020 Belgrade, Serbia, E-mail: ignjatovic@etf.rs

Jovan Cvetić is with the School of Electrical Engineering, University of Belgrade, 73 Bulevar kralja Aleksandra, 11020 Belgrade, Serbia, E-mail: cvetic_j@etf.rs

Dragan Pavlović is with the School of Electrical Engineering, University of Belgrade, 73 Bulevar kralja Aleksandra, 11020 Belgrade, Serbia, E-mail: dragan.lab3@etf.rs

The main goal of the paper is to numerically simulate the propagation of the overvoltage wave along the transmission line including the corona. The effect of corona is taken into consideration by the drift-diffusion-reaction model which represents the set of the continuity equations for each type of particles (electrons, positive and negative ions, neutrals, etc.) that participate in the discharge. The model enables the inclusion and the analysis of detailed physical and chemical reactions that are taking place in the area around the wire of the transmission line.

## II. THEORY

### *A. Transmission Line Equations*

The equations describing voltage and current along the overhead wire taking into account the effect of corona [4] are

$$\frac{\partial V(t,x)}{\partial x} + L\frac{\partial I(t,x)}{\partial t} = 0, \tag{1}$$

$$\frac{\partial I(t,x)}{\partial x} + \frac{\partial Q(t,x)}{\partial t} = 0. \tag{2}$$

These equations represent telegrapher's equations for lossless transmission line where $Q(t,x)$ is the total line charge density. In vacuum, the charge-voltage dependence is linear $Q(t,x) = CV(t,x)$. The inductance and the capacitance per line length, $L$ and $C$ respectively, can be calculated by formula

$$L = \frac{\mu_0}{2\pi}\operatorname{acosh}\left(\frac{h}{a}\right),\ C = 2\pi\varepsilon_0 \Big/ \operatorname{acosh}\left(\frac{h}{a}\right), \tag{3}$$

where $a$ is the wire radius and $h$ is the height of the wire above the ground.

When the voltage intensity is greater than the critical value for the corona inception, the charge voltage dependence becomes nonlinear with the hysteresis. This function is represented by charge-voltage (QV) curve. In order to study the pulse propagation, it is necessary to know the accumulated charge on the transmission line for the given voltage when corona is formed and to determine the QV curve for every position along the transmission line. For the given time evolution of voltage at some position along the line $V(t,x)$, one can obtain the total line charge density $Q$ by solving the continuity equations for charged species in air in cylindrical geometry [5].

*B. Drift-Diffusion Model for Corona*

In this study, we take into consideration the concentration of electrons $n_e$, positive ions $n_p$, negative $O^-$ and $O_2^-$ ions, $n_{O^-}$ and $n_{O_2^-}$, respectively.

$$\frac{\partial n_e}{\partial t}+\frac{1}{r}\frac{\partial\left(r\Gamma_e\right)}{\partial r}=S_{ph}+n_e(\alpha-\eta_2-\eta_3)\left|W_e\right|-n_e n_p\beta+k_{\text{det}}n_{O_2^-}, \tag{4}$$

$$\frac{\partial n_p}{\partial t}+\frac{1}{r}\frac{\partial\left(r\Gamma_p\right)}{\partial r}=S_{ph}+n_e\alpha\left|W_e\right|-(n_e+n_{O^-}+n_{O_2^-})n_p\beta, \tag{5}$$

$$\frac{\partial n_{O^-}}{\partial t}+\frac{1}{r}\frac{\partial\left(r\Gamma_{O^-}\right)}{\partial r}=n_e\eta_2\left|W_e\right|-n_{O^-}n_p\beta, \tag{6}$$

$$\frac{\partial n_{O_2^-}}{\partial t}+\frac{1}{r}\frac{\partial\left(r\Gamma_{O_2^-}\right)}{\partial r}=n_e\eta_3\left|W_e\right|-n_{O_2^-}n_p\beta-k_{\text{det}}n_{O_2^-}. \tag{7}$$

On the right hand side of the equations (4)-(7) the terms representing the gain and the loss of the particles due to electron impact ionization, two-body attachment, three-body attachment, recombination and detachment described by the coefficients $\alpha$, $\eta_2$, $\eta_3$, $\beta$ and $k_{\text{det}}$ respectively are given. The term $S_{ph}$ denotes the generation of electrons and positive ions through photoionization. Further, $W_e$, $W_p$ and $W_n$ are the velocities of electrons, positive and negative ion drifts, respectively. The fluxes of charged particles are given by

$$\Gamma_e=W_e n_e-D\frac{\partial n_e}{\partial r},\ \Gamma_p=W_p n_p,\ \Gamma_{O^-}=W_n n_{O^-},\ \Gamma_{O_2^-}=W_n n_{O_2^-}, \tag{8}$$

where $\Gamma_e$ is the flux of electrons, $\Gamma_p$ is a flux of positive ions, $\Gamma_{O^-}$ and $\Gamma_{O_2^-}$ are the fluxes of $O^-$ and $O_2^-$ ions, respectively, $D$ is the diffusion coefficient for electrons. We neglected the diffusion of heavy ions, so the ionic current contains only a drift component.

The concentration of positive ions consists mainly from $N_2^+$ and $O_2^+$ ions generated by electron impact ionization and photoionization. The negative $O^-$ and $O_2^-$ ions are treated separately in order to take into account the process of detachment of electrons from $O_2^-$ ions due to collisions with $O_2$ molecules [6]. Moreover, these two negative ions are generated by two different attachment processes in air [7]. For higher values of the electric field intensity, the most significant attachment process is two-body dissociative attachment

$$\mathrm{e}+\mathrm{O_2}\rightarrow\mathrm{O^-}+\mathrm{O}, \tag{9}$$

so the negative $O^-$ ions are produced. The $O_2^-$ ions are produced in the three-body attachment process

$$\mathrm{e}+\mathrm{O_2}+\mathrm{M}\rightarrow\mathrm{O_2^-}+\mathrm{M}, \tag{10}$$

which is the dominant process at low values of the electric field.

The photoionization term $S_{ph}$ is calculated by using the model of Zheleznyak [8] and the details about the calculation in cylindrical geometry are given in [9]. The values of the transport and the reaction coefficients are adopted from [10] and they depend on the ratio of the value of the electric field intensity and the concentration of air molecules, so the continuity equations (4)-(7) are coupled with the Poisson equation using the potential $\Phi$

$$\nabla^2\Phi=\frac{1}{r}\frac{\partial}{\partial r}\left(r\frac{\partial\Phi}{\partial r}\right)=-\frac{e\left(n_p-n_e-n_{O^-}-n_{O_2^-}\right)}{\varepsilon_0}. \tag{11}$$

Electric field is calculated assuming the electrostatic approximation

$$E=-grad\ \Phi=-\frac{\partial\Phi}{\partial r}. \tag{12}$$

*C. Boundary Conditions and the Processes at the Cathode*

The radii of the central wire and the outer cylinder are $R_1$ and $R_2$, respectively. One needs to define boundary conditions for the system of partial differential equations (4)-(7) and (11). Since the voltage impulse is applied to the central electrode, while the outer cylinder is grounded, the boundary conditions for the Poisson equation (11) are

$$\Phi(r=R_1)=V(t),\ \Phi(r=R_2)=0, \tag{13}$$

where $V(t)$ is the value of the applied voltage at time *t*. As for the continuity equations (4)-(7) the boundary conditions at the central electrode are important, because all the significant processes during the discharge take place in the vicinity of the wire. For the configuration examined in this study, the outer cylinder is far enough from the wire, so the electric field in this region does not reach the critical value for the ionization. Since the concentrations of the charged particles at the outer boundary are negligible during the discharge, the simulation does not depend on the boundary conditions at the outer cylinder. We adopted the condition that the concentrations of the charged particles at $r=R_2$ have zero value

$$n_e(r=R_2)=n_p(r=R_2)=n_{O^-}(r=R_2)=n_{O_2^-}(r=R_2)=0. \tag{14}$$

Another effect that must be taken into account for the negative corona discharge is the emission of the electrons from the cathode due to photoemission and positive ion impact. Both effects can be included in the simulation through the boundary conditions for electrons at the cathode

$$n_e(r=R_1)=n_{ei}+n_{eph}, \tag{15}$$

where $n_{ei}$ and $n_{eph}$ denote the terms due to positive ion impact and photoemission, respectively. The ratio of the fluxes of emitted electrons and incident positive ions is equal to the ion-secondary emission coefficient $\gamma_i$, so one obtains

$$n_{ei}=\gamma_i\frac{\left|W_p(r=R_1)\right|}{\left|W_e(r=R_1)\right|}n_p(r=R_1). \tag{16}$$

The term $n_{eph}$ is calculated by the extended model of Aleksandrov [11,12]:

$$n_{eph}=\frac{\gamma_{ph}}{\left|W_e\left(r=R_1\right)\right|}\int_{R_1}^{R_2}\alpha n_e\left|W\right|_e g\left(r\right)e^{-\mu(r-R_1)}\frac{r}{R_1}dr, \tag{17}$$

Where $\gamma_{ph}$ is photoemission coefficient, $\mu=6\ \mathrm{cm}^{-1}$ is absorption coefficient for photons in air and $g(r)$ is geometrical factor given by

$$g\left(r\right)=g_{radial}\left(r\right)\cdot g_{axial}\left(r\right) \tag{18}$$

$$g_{radial}\left(r\right)=\frac{1}{\pi e^{-\mu(r-R_1)}}\int_0^{\sin^{-1}(R_1/r)}e^{-\mu\left(R_1^2+r^2-2R_1r\cos\varphi\right)^{\frac{1}{2}}}d\varphi \tag{19}$$

$$g_{axial}\left(r\right)=\frac{2}{\pi e^{-\mu(r-R_1)}}\int_0^{\pi/2}e^{-\mu(r-R_1)/\cos\varphi}d\varphi \tag{20}$$

The values of secondary emission coefficients are adopted to be $\gamma_i=0.01$ [13] and $\gamma_{ph}=0.0015$ [14].

As for the boundary conditions for the ions concern, we adopted the assumption that both the positive and the negative ions can leave the system through the central wire defining Neumann boundary conditions. This is necessary because the simulation shows that the central electrode changes its polarity during the discharge, although the applied voltage keeps the negative value during the whole discharge process. Finally, the boundary conditions at the central wire are

$$\left.\frac{\partial n_p}{\partial r}\right|_{r=R_1}=\left.\frac{\partial n_{O^-}}{\partial r}\right|_{r=R_1}=\left.\frac{\partial n_{O_2^-}}{\partial r}\right|_{r=R_1}=0. \tag{21}$$

For the mathematical completion of the equations, one still needs to define the initial conditions for the concentrations of the charged particles. Under the standard conditions for temperature and pressure air is excellent insulator. However, there are always some seed electrons generated due to cosmic radiation, natural radioactivity and other phenomena, so about 10 electron-ion pairs are produced in $1\ \mathrm{cm}^3$ per $1\ \mathrm{s}$. In the absence of strong electric field free electrons exist only for a very short time due to the attachment to oxygen molecules and the steady-state number of positive and negative ion pairs is about 1000 per $1\ \mathrm{cm}^3$. Therefore, we adopted that there are initially 1000 positive and negative $O_2^-$ ion pairs per cubic centimeter [15] and the initial concentrations of the electrons and $O^-$ ions have zero value

$$\begin{aligned} &n_p(t=0)=n_{O_2^-}(t=0)=10^9\ \mathrm{m}^{-3},\\ &n_e(t=0)=n_{O^-}(t=0)=0. \end{aligned} \tag{22}$$

For the sake of the simplicity we adopted the assumption that at the time onset the concentrations of the charged particles are uniform all over the interelectrode space. The seed electrons needed for the avalanche multiplication will be generated through emission from the cathode or by detachment from negative $O_2^-$ ions. In reality, there will be a certain time delay of the corona inception. This ignition time lag corresponds to the production of the seed electron, which is a stochastic event. In this study, time lag is neglected since it decreases considerably with the increase of humidity in air, which is the case for the atmospheric conditions during the lightning.

For solving the continuity equations (4)-(7) numerically, we used the flux-corrected transport (FCT) algorithm. We followed the approach described by Book, Boris and Zalesak [16]. The Poisson equation is solved by finite-difference method. Since the electric field changes abruptly in the vicinity of the wire, one needs to introduce very fine computational mesh in this region. In the region towards the outer cylinder mesh can be more coarse and one would have less steps for computation and time of the computation will be shorter. Time step should be chosen considering the motion of electrons, since they are the fastest particles. The total time of the simulation is 50 μs and it is equally divided into $10^7$ time steps.

## III. Results and Discussion

When the concentrations of the charge particles and the electric field intensity are calculated, the total line charge density is

$$Q(t)=\int_0^t I_p(t')dt', \tag{23}$$

where $I_p$ is the current per cylinder length, obtained from Sato-Morrow [17] formula for cylindrical geometry

$$I_p=\frac{2\pi e}{\log\frac{R_2}{R_1}}\int_{R_1}^{R_2}\Gamma dr+\frac{2\pi\varepsilon_0}{\log\frac{R_2}{R_1}}\frac{\partial V}{\partial t}. \tag{24}$$

Final goal is to investigate whether the drift-diffusion model in the cylindrical geometry can be used for the simulation of QV curves for the overvoltage calculations in different geometry for transmission lines. Noda [18] measured the QV curves for the overhead wire 1.83 m above the ground. In order to try to estimate the QV curve measured by Noda in wire to plane geometry we ran the simulation in our wire to cylinder program. The radius of the wire is same as in the experiment, $R_1 = 5$ mm , and the radius of the outer cylinder is adopted to be the height of the wire above the ground, which is $R_2 = 1.83$ m . Calculated values for the total line charge density were higher than the measured values, which is expected since the capacitance of the cylindrical capacitor is greater than the capacitance of the wire above the perfectly conducting plane. Therefore, the result for the line charge density should be multiplied by the coefficient $k$, which is the ratio of the capacitance of the wire above the plane $C_p$ and the capacitance of the cylindrical capacitor $C_0$

$$C_p = \frac{2\pi\varepsilon_0}{\cosh^{-1}\left(R_2/R_1\right)},\ k = \frac{C_p}{C_0}. \tag{25}$$

In this way, we obtained a very good agreement with the experimental results. The QV curve obtained by the correction of the calculated results and the data measured by Noda for 570 kV impulse are depicted in Fig. 1.

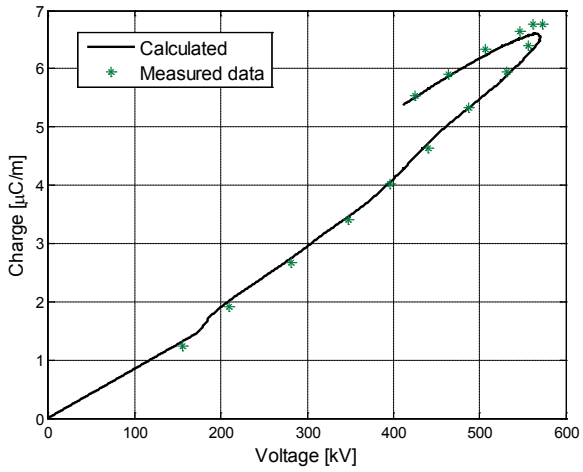


Fig. 1. Calculated QV curve and the measured data by Noda [18]

The final result of the simulation shows excellent agreement with the experimental measurement of the QV curve. It represents affirmation that the drift diffusion model can be used for the calculation of QV curves, which are necessary to complete the equations (1) and (2) in order to study the pulse propagation along the transmission line.

In order to solve the equations (4)-(7) and (11) numerically, great number of time steps is necessary. For the simulation of the 5 μs corona discharge, a million time steps is needed. Therefore, it would be very time consuming to simulate the corona at every position along the transmission line. So, the corona discharge is simulated only on some nodes along the line and the values between those nodes are obtained by linear interpolation.

The calculations of the surge propagation have been performed for the single overhead wire of the radius $a = 21$ mm placed at the height $h = 15$ m above the ground. The goal is to try to obtain the same results as in the experiments preformed by Wagner et al [19]. The surge generator was located at the one end of the line and the voltage pulse is injected which defines the boundary condition $V(x = 0, t)$ . Since the pulse can not propagate with the speed greater then the speed of light, two more boundary conditions can be defined $I(x > ct) = 0,\ V(x > ct) = 0$ .

The surge generator voltage impulse and the shape of the voltage impulse after the wave travelled the distance of 622 m are given in the Fig. 2. Unfortunately, first result of the simulation did not give the solution that has satisfactory agreement with the measured impulse. On a positive note, simulation confirmed all effects of the corona- the retardation and the attenuation of the impulse and correct value of the corona threshold.

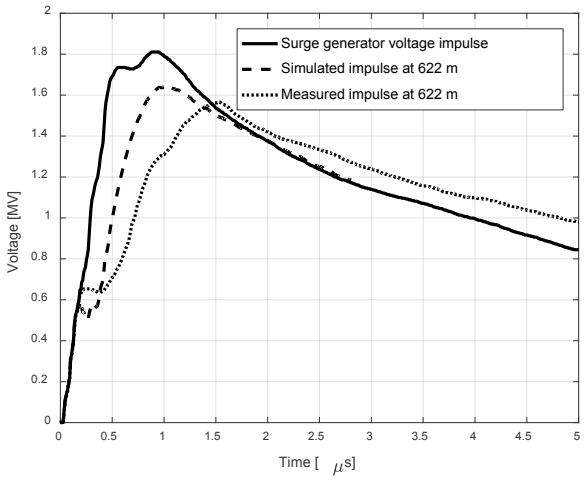


Fig. 2. Simulation of the propagation of the surge pulse at 622 m

In order to obtain better results, we conducted the investigation why results are different. By comparing results of the QV curves with the engineering models it was concluded that drift-diffusion model gives lower values of the charge for wires with the radius greater than 10 mm. The comparisons of the simulated QV curves with the result of CIGRE parabolic model are presented in the Figs. 3 and 4. There is significant difference between the results for the wire radius of 21 mm (Fig 4.). On the other hand, for thinner wires drift-diffusion model gives satisfactory solution, as shown in Figs. 1 and 3. Therefore, in our example the generated charge is less than it should be and corona effect is not strong enough to obtain agreement with the measured values.

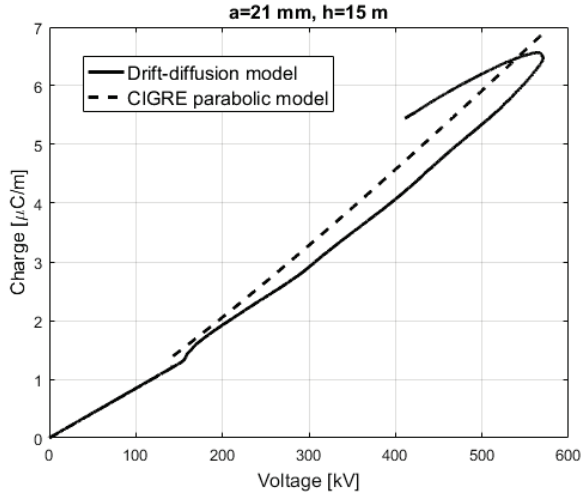


Fig. 3. Comparison of the QV curves calculated by the drift-diffusion model and by the CIGRE parabolic model for the wire radius of 5 mm

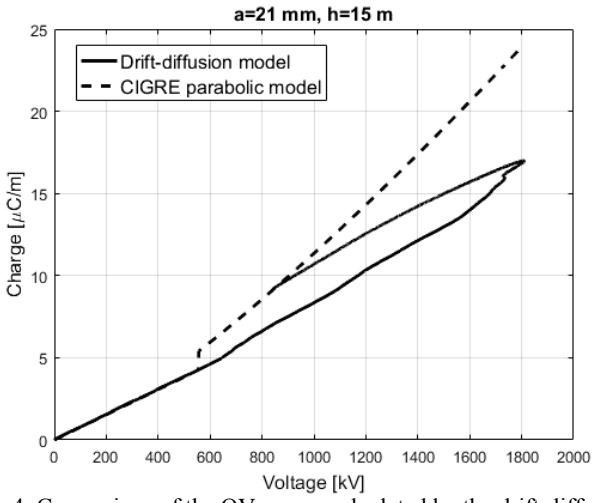


Fig. 4. Comparison of the QV curves calculated by the drift-diffusion model and by the CIGRE parabolic model for the wire radius of 21 mm

This difference in the results for the thin and wide wires can be explained by the effect of streamer. The structure of the space charge around the wire is not the radially symmetrical fluid, as it is assumed by drift-diffusion model. In reality, the space charge is composed of thin filaments of the discharge – the streamers. These filaments have the head where photoionization occurs and they propagate through space leaving behind the weakly ionized tail [15]. Their significant characteristic is that they can propagate even when the electric field intensity is smaller than the critical electric field for the impact ionization (around 2.6 MV/m for dry air). This is possible because very high intensity electric field is generated in the head of the streamer and photons that further ionize molecules are emitted. The minimal value of the electric field for the propagation of the positive streamers is 0.5 MV/m, and for the negative streamers it is around 1 MV/m.

Due to streamers additional charge is generated in the area farther form the wire where the electric field has lower intensity values, which can not be taken into account with the original drift-diffusion model. In order to include this effect, we modified the values of the Townsend coefficient $\alpha$ which represents the number of positive ion-electron pairs generated per unit length. For the atmospheric pressure, the Townsend coefficient depends only on the electric field intensity. The modification is done so that the Townsend coefficient has values high enough for the ionization when the electric field intensity is lowered to 1 MV/m. Adopted values for the Townsend coefficient are given in Fig. 5. The calculations showed that important parameter of modification is the minimal electric field for the ionization to occur. On the other hand, if the value of the Townsend coefficient in this range is greater, it does not affect the results of the simulation. This procedure gave the result that is in a good overall agreement with the experimental results, as can be seen in Fig. 6.

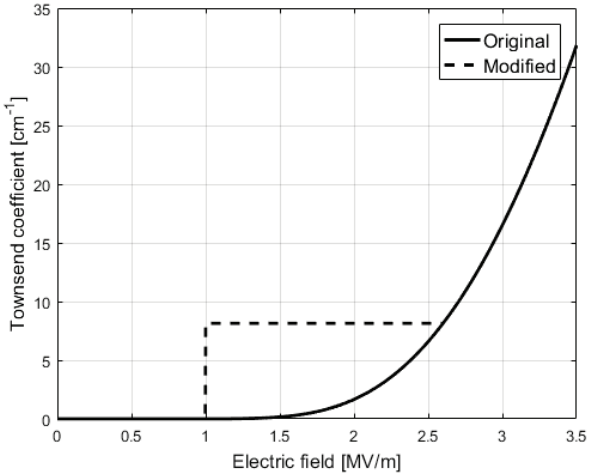


Fig. 5. Values of Townsend coefficient dependent on the electric field intensity

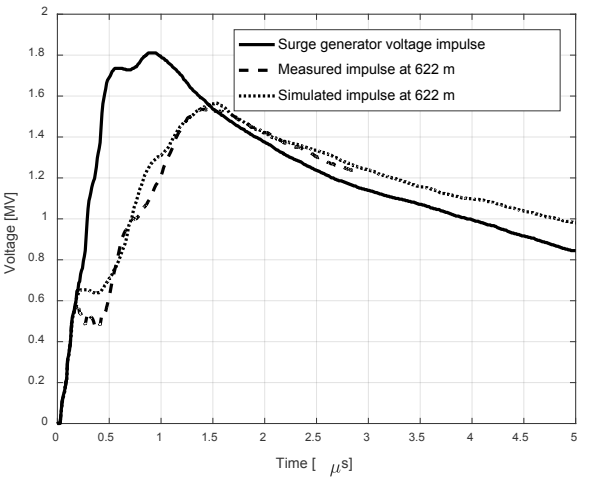


Fig. 6. Simulation of the propagation of the surge pulse at 622 m with the modified Townsend coefficient value

## IV. CONCLUSION

The drift-diffusion model has been used to simulate corona discharge due to lightning surge on transmission lines. In order to obtain a good agreement with the experimental results, reaction coefficient for the impact ionization needs to

be modified. It is necessary to include the effect of the streamers, the thin filaments of the discharge that can propagate in the area of lower electric field intensity. The streamers increase the generated charge around the wire and enhance the effects of the corona.

## ACKNOWLEDGEMENT

Ministry of Science and Technological Development of the Republic of Serbia supported this work under contracts No. 171007 and 37019.

This is an extended version of the paper "The Influence of Corona on the Lightning Surge Propagation Along Transmission Lines" presented at the 6th International Conference on Electrical, Electronic and Computing Engineering IcETRAN 2019, held in June 2019 on Silver Lake, Serbia. The paper has been awarded as the best paper presented in the Section Antennas and Propagation.

## REFERENCES

[1] A.R. Hileman, *Insulation Coordination for Power Systems,* Boca Raton, USA, Taylor & Francis, 1999.

[2] K.H. Weck and A.J. Eriksson, "Simplified Procedures for Determining Representative Substation Impinging Lightning Overvoltages", *CIGRE,* Paper 33-16, 1988.

[3] F.W. Peek, *Dielectric Phenomena in HV Engineering,* McGraw-Hill, 1929.

[4] V. Cooray and N. Theethayi, "Pulse Propagation Along Transmission Lines in the Presence of Corona and Their Implication to Lightning Return Strokes", *IEEE Transactions on Antennas and Propagation*, vol. 56, no. 7, pp. 1948-1959, July 2008.

[5] A. Luque and U. Ebert, "Density Models for Streamer Discharges: Beyond Cylindrical Symmetry and Homogenous Media", *Journal of Computational Physics*, vol. 231, 2012, pp. 904-918.

[6] A.A. Ponomarev and N.L. Aleksandrov, "Monte Carlo Simulation of Electron Detachment Properties for $O_2^-$ Ions in Oxygen and Oxygen:Nitrogen Mixtures", *Plasma Sources Sci. Technol.*, vol 24, no. 3, 03501, 2015.

[7] S. Pancheshnyi, "Effective Ionization Rate in Nitrogen-Oxygen Mixtures", *J. Phys. D: Appl. Phys.*, vol. 46, no. 15, 155201, 2013.

[8] M.B. Zhelezniak, A.K. Mnatsakanian, and S.V. Sizykh, "Photoionization of Nitrogen and Oxygen Mixtures by Radiation from a gas Discharge", *High. Temp.*, vol. 20, pp. 367-362, 1982.

[9] A.A. Kulikovsky, "The Role of Photoionization in Positive Streamer Dynamics", *J. Phys. D: Appl. Phys.*, vol. 33, no. 12, pp. 1514-1524, 2000.

[10] R. Morrow and J.J. Lowke, "Streamer Propagation in Air", *J. Phys. D: Appl. Phys.*, vol. 30, pp. 614-627, 1997.

[11] G.N. Aleksandrov, "Physical Conditions for the Formation of an Alternating Current Corona Discharge", *Soviet Phys. Tech. Phys.*, pp. 1714-1726, 1956.

[12] Y. Zheng, J. He, B. Zhang, R. Zeng, and Z. Yu, "Surface Electric Field for Negative Corona Discharge in Atmospheric Pressure Air", *IEEE Transactions on Plasma Science*, vol. 39, no. 8, pp. 1644-1651, 2011.

[13] R. Morrow, "Theory of Negative Corona in Oxygen", *Physical Review A*, vol. 32, no. 3, pp. 1799-1809, Sept. 1985.

[14] J. Chen and J. Davidson, "Model of the Negative DC Corona Plasma: Comparison to the Positive DC Corona Plasma", *Plasma Chemistry and Plasma Processing*, vol. 23, no. 1, pp. 83-102, 2003.

[15] Y. Raizer, *Gas Discharge Physics*, Springer-Verlag, Berlin, Germany, 1991.

[16] D.L. Book, J.P. Boris, and S.T. Zalesak, "Flux-Corrected Transport" in *Finite-Difference Techniques for Vectorized Fluid Dynamics Calculations*, New York, Springer, 1981, ch. 3, pp. 29-55.

[17] R. Morrow and N. Sato, "The Discharge Current Induced by the Motion of Charged Particles in Time-Dependent Electric Fields; Sato's Equation Extended", *J. Phys. D: Appl. Phys*, vol. 32, pp. L20-L22, 1999.

[18] T. Noda, T. Ono, H. Matsubara, H. Motoyama, S. Sekioka and A. Ametani, "Charge-Voltage Curves of Surge Corona on Transmission Lines: Two Measurement Methods", *IEEE Transactions on Power Delivery*, vol. 18, no. 1, pp. 307-314, Jan. 2003.

[19] C.F. Wagner, I.W. Gross, and B.L. Lloyd, "High-Voltage Impulse Tests on Transmission Lines", *AIEE Trans.*, 1954, pp. 196-210.